Electrodisintegration of the Deuteron Around $q^2=3.5\ \mathrm{F}^{-2}$

B. GROSSETÊTE, S. JULLIAN, AND P. LEHMANN
Ecole Normale Supérieure, Laboratoire de l'Accélérateur Linéaire, Orsay, France.
(Received 29 April 1965)

We have measured the absolute cross sections of the electron-deuteron scattering at $q^2=3.5\ \mathrm{F}^{-2}$ and obtained the complete inelastic spectrum. Three points for each spectrum are given with a 4% accuracy. The scattering angles, 60° and 130°, were chosen to allow the separation between electric and magnetic scattering. Calculations of radiative corrections were made in order to permit the comparison of the spectra with the inelastic-scattering theories.

I. INTRODUCTION

WE present here the experimental results obtained at Orsay on inelastic electron-deuteron scattering. The aim of these experiments is to obtain results permitting the study of the electrodisintegration mechanism. For this reason, our measurements are not limited to the cross section at the top of the inelastic peak, but concern also the whole spectra of the scattered electrons from the threshold to some 10 MeV below the peak. In three characteristic regions of each spectrum, one point has been taken with a better accuracy. The following article[1] gives a comparison of experimental cross sections with theoretical predictions of nonrelativistic theories.

The experiments have been performed in the 500-MeV experimental area of the linear electron accelerator at Orsay. It has been possible to measure the cross section around $q^2=3.5\ \mathrm{F}^{-2}$. In this range of q^2, the nonrelativistic theory is expected to be valid and is very sensitive to the final-state interactions of the outgoing neutron-proton system. This experiment permits the choice of the theory most suitable to the final-state interaction.

Our measurements have been taken at two different angles, 60° and 130°. The first corresponds to a 60% electric scattering and the second to an essentially magnetic scattering (80%). Because of the known angular dependence of the cross section, similar to that of the Rosenbluth formula, measurements at other angles are not necessary.

II. APPARATUS

The general aspect of the apparatus has already been described several times, particularly in the previous paper discussing the elastic-scattering experiment performed in the 250-MeV room of the accelerator.[2] Only the specific problems related to the 500-MeV room will be mentioned here.

(1) Target

The same liquid hydrogen or deuterium target used for the elastic scattering is used here. It is an aluminum cylinder of revolution (diameter: 2.2 cm; thickness of the walls: 40 μ). The axis is oriented perpendicularly to the beam. The thickness of liquid hydrogen or deuterium is very well known (0.5%). Because of the cylindrical shape of the target, no warping (under 2 kg/cm^2 pressure) was observed using a transit. Deuterium or hydrogen temperature was measured to be +0.1° above that of the cryostat. This target enabled us to take absolute measurements, as confirmed by the results on the elastic electron-proton scattering performed during this experiment (Sec. III).

(2) Spectrometer

The double-focusing spectrometer was calibrated using the floating-wire method, giving results reproducible within 0.2%; however we give a 0.5% error in order to include the systematic errors.

The dispersion has been measured for several momenta by means of the floating wire, and is a constant for the experiment within a range of 1%. The solid angle is limited by a slit of tungsten at the spectrometer input. Its value is 3×10^{-3} sr. Experiments studying the elastic tail of the proton have shown that the edge effects are insignificant in the case of the inelastic electron-deuteron scattering in this range of q^2.[3] A slit of tungsten, placed at the output of the spectrometer, defines the momentum range of the scattered electron. We have chosen a momentum range of approximately 3 MeV, which is small compared with the width of the inelastic peak. (The half-height width of the inelastic peak is 40 MeV).

(3) Čerenkov Counter

The scattered electrons are counted by means of a Lucite Čerenkov counter (17 cm×12 cm×14 cm) and a photomultiplier (Dario 58 A V P). The electron Čerenkov peak is narrow enough to differentiate it from the π-meson Čerenkov peak (Fig. 1). For kinematical reasons the π creation threshold was not reached for the scattering at 130°; even at 60° the π meson appeared only over a certain range of inelastic spectra. It was not necessary to design a special system allowing rejection π mesons. The correction, when necessary, was obtained

[1] B. Bosco, B. Grossetête, and P. Quarati, following paper, Phys. Rev. **141**, 1441 (1966).
[2] B. Grossetête, D. J. Drickey, and P. Lehmann, preceding paper, Phys. Rev. **141**, 1425 (1966).
[3] P. Emsalem, Diplôme d'Etudes Supérieures, Orsay, Linear Accelerator Laboratory Report No. L.A.L. 1106, 1964 (unpublished).

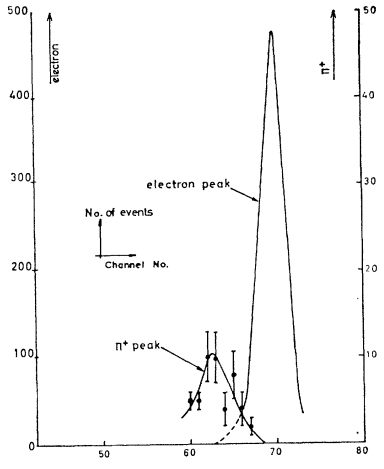

FIG. 1. Comparison of pulses given by pions and electrons of same momentum (339 MeV/c) in a Čerenkov counter. Pion data are obtained by reversing the spectrometer field.

by studying the Čerenkov spectrum. Their speed being less, π mesons give less light than electrons of the same momentum (Fig. 1). The π contribution was less than 2%.

(4) Electronics

The Čerenkov pulses are analyzed by slow electronics. We count one event per beam pulse. The counting losses have been calculated using the intensity distribution of accelerator pulses given in an auxiliary counter. The incident electron beam is measured by a secondary-electron monitor calibrated against a Faraday cup.

(5) Background

In order to obtain the background of the experimental area and of the target walls, we perform empty-target measurements and with the filled target we analyze momenta larger than those of the elastic peak of the deuteron. Some background is produced by electrons with momenta different from those of the analyzed electrons. These electrons are scattered by the spectrometer chamber and give a Čerenkov signal smaller than the one given by the scattered electrons. Evaluation of this background was obtained by studying the Čerenkov spectrum.

III. ELECTRON-PROTON SCATTERING

In order to make sure that the cross-sections were absolute, we measured the proton form factors for nearby energies during the two runs of this experiment. The results (Table I and Fig. 2) agree with other measurements obtained at Stanford[4] and Orsay.[5]

We assume that $F_p{}^c = F_p{}^m = F_p$. This is in agreement with the proton measurements of Dudelzak.[5]

IV. UNCORRECTED RESULTS

Six spectra have been taken: four at 60°, where the cross-section is 60% electric, and two at 130°, where it is essentially magnetic (80%).

The measurements before correction in arbitrary units are shown in Fig. 3. Some points have been measured with a better accuracy (i.e., with better statistics). Those situated near threshold, or at half height of the quasi-elastic peak, may be used to determine Bosco's constants[1]; those situated at the top of the peak are used in order to determine neutron form factors. For all these measurements numerous tests have been made (energy determination, monitor efficiency, beam position, etc.). One point at the top of the inelastic peak (404 MeV, $\theta = 60°$) has been rejected because of the possible hydrogen impurity and consequent overlapping of the quasi-elastic peak by the proton peak.

V. DEUTERON CORRECTIONS

The study of the elastic tail of the proton under the same experimental conditions[3] has shown that corrections[6] are due to (1) radiative effects, (2) bremsstrahlung

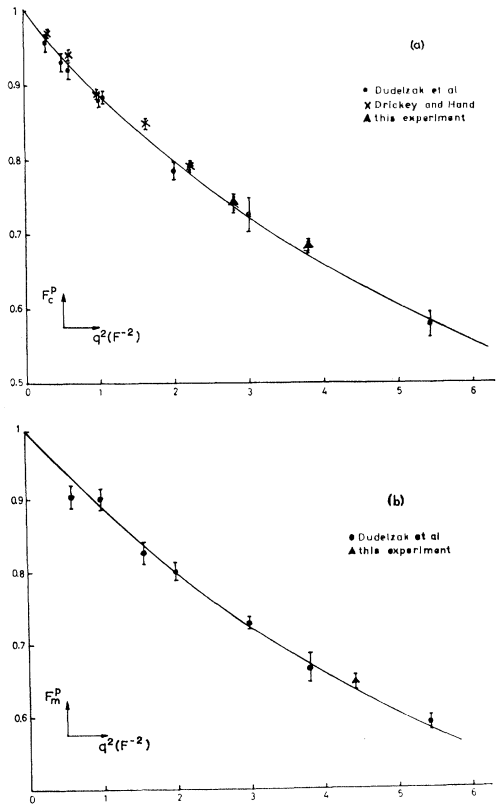

FIG. 2. Comparison of proton form factors measured during this experiment with those of Dudelzak *et al.* (Ref. 5) and of Drickey and Hand (Ref. 4).

[4] D. J. Drickey and L. N. Hand, Phys. Rev. Letters **9**, 521 (1962).

[5] B. Dudelzak and P. Lehmann, in *Proceedings of the Sienna International Conference on Elementary Particles, 1963*, edited by G. Bernadini and G. P. Puppi (Società Italiana di Fisica, Bologna, 1963), Vol. 1, p. 495.

[6] This problem is more completely described in B. Grossetête, thesis [Orsay Linear Accelerator Laboratory Report No. L.A.L. 1113, 1964 (unpublished)].

TABLE I. Proton data and corrections.

Incident energy (MeV)	Scattering angle (deg)	q^2 (F^{-2})	Ionization correction	Bremsstrahlung correction	Tsai radiative correction	$d\sigma/d\Omega$ (experimental, corrected) (cm^2)	F_p
426.0	60	3.79	1.011	1.041	1.213	$(1.95\pm0.05)10^{-31}$	0.683 ± 0.008
359.0	60	2.79	1.010	1.041	1.210	$(2.98\pm0.06)10^{-31}$	0.736 ± 0.009
279.4	130	4.43	1.018	1.041	1.227	$(2.37\pm0.06)10^{-31}$	0.648 ± 0.008

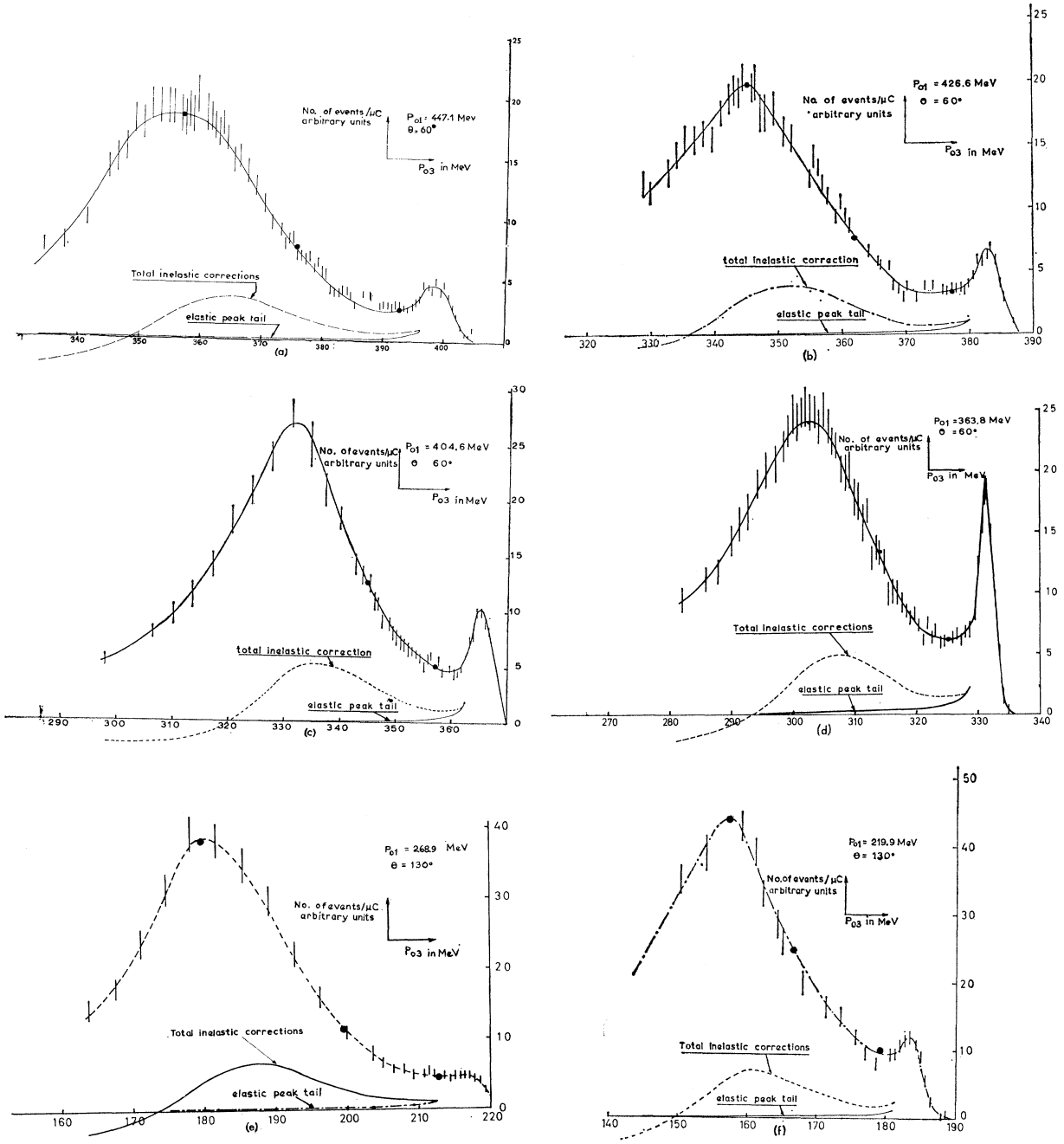

FIG. 3. Deuteron data. The more accurate points are represented by a dot. For the others, statistical errors are indicated. A smooth curve is drawn across all points. Corrections to the cross sections are given by two curves.

TABLE II. Thickness crossed by the electrons scattered in the middle of the target.

Scattering angle (deg)	Thickness (g/cm²)	Thickness (radiation lengths)
60	0.690	0.0087
130	0.603	0.0077

on nucleus different from the scattering nucleus, and (3) ionization.

Only the radiative corrections need to be calculated exactly; because of the small thickness crossed by the electrons (Table II) the two last effects may be calculated approximately.

Including radiative corrections the cross sections can be expressed as

$$\frac{d^2\sigma}{d\Omega dp_{03}}(p_{01},p_{03})=\int_0^{k_{\max}}\frac{d^3\sigma}{d\Omega dp_{03}dk}(p_{01},p_{03},k)dk,$$

where p_{01} and p_{03} are, respectively, the energy of the incident and scattered electrons, and k is the momentum of the photon emitted.

Assuming that the high-energy photons are emitted in the direction of the electron before or after scattering, the cross section becomes the probability of emitting one photon (of energy k) times the scattering probability of the electron:

$$\frac{d^2\sigma}{d\Omega dp_{03}}(p_{03})=\int_0^{k_{i\max}}f_i(k)\frac{d^2\sigma}{d\Omega dp_{03}}(p_{01}+k,\,k)dk+\int_0^{k_{f\max}}f_f(k)\frac{d^2\sigma}{d\Omega dp_{03}}(p_{01},\,p_{03}+k)dk.$$

The problem is to determine $d^2\sigma/d\Omega dp_{03}$, which is the final result. We have to solve an integral equation. To do so we must find the cross section for all energies of the electrons before and after scattering at the same angle. Without the above approximation it would have been necessary to introduce cross sections at all angles.

Using the method of Meister *et al.*,[7] we divide the integration interval into two parts:

$$0<k<5\text{ MeV},$$
$$5\text{ MeV}<k<k_{\max}.$$

The first part corresponds to the emission of soft photons, and the second part to hard photons. The soft-photon calculation is the same as in elastic scattering. We have taken the Meister-Yennie formula[8] for elastic radiative corrections.

The hard-photon contribution was calculated numerically, supposing that the inelastic cross section was known and using for $f_i(k)$ and $f_f(k)$ Meister's formula.[7] For the inelastic cross-section we used Durand's formula and introduced the final-state interaction in the S wave.

The calculated theoretical spectra obtained by means of this method fit the experimental spectra with an accuracy better than 10% on the complete spectra for all energies and angles. Thus the calculation of the hard-photon part is good to within 10%. The contribution of hard photons between the threshold and the top of inelastic peak is less than 10%. Consequently the net uncertainty is smaller than 1%. In the low-energy region of the inelastic peak, the contribution of the hard photons becomes more important and gives a greater error.

In conclusion, it was not necessary to solve integral

TABLE III. Numerical results for the points taken with a better accuracy.

Incident energy p_{01} (MeV)	Scattering angle θ (deg)	Scattering energy p_{03} (MeV)	$d^2\sigma/d\Omega dp_{03}$ uncorrected (10^{-33} cm²)	Elastic contribution (10^{-33} cm²)	Total correction	Hard-photon contribution	$d^2\sigma/d\Omega dp_{03}$ corrected (10^{-33} cm²)	Statistical error (%)	Total error (%)
447.1	60	392.7	0.586	0.082	1.290	···	0.651	2.2	5.0
		375.7	1.887	0.025	1.285	0.036	2.392	1.4	4.0
		356.7	4.699	0.016	1.118	0.085	5.30	1.6	3.8
426.6	60	377.2	0.833	0.123	1.293	···	0.918	2.2	5.0
		361.9	2.030	0.036	1.290	0.032	2.576	1.8	3.9
		345.3	5.483	0.023	1.160	0.062	0.334	1.6	3.9
404.6	60	357.0	1.210	0.124	1.268	0.019	1.387	1.7	4.5
		344.6	3.109	0.054	1.286	0.033	3.928	1.4	3.8
363.8	60	325.3	2.113	0.310	1.275	···	2.298	2.1	4.6
		314.2	4.801	0.120	1.278	0.028	5.982	1.7	3.6
		302.6	8.799	0.077	1.159	0.051	10.11	1.6	3.5
268.9	130	212.9	0.0993	0.0070	1.228	···	0.1139	3.2	4.9
		200.1	0.2703	0.0019	1.245	0.029	0.3341	1.8	3.2
		180.0	0.9953	0.0014	1.115	0.056	1.1092	1.6	3.1
219.9	130	179.2	0.3471	0.0196	1.220	···	0.3995	2.3	4.2
		166.7	0.9159	0.0003	1.228	0.020	1.117	1.9	3.5
		157.3	1.6904	0.0049	1.130	0.042	1.905	2.0	3.5

[7] N. T. Meister and T. A. Griffy, Phys. Rev. **133**, B1032 (1964).
[8] N. T. Meister and D. R. Yennie, Phys. Rev. **130**, 1210 (1963).

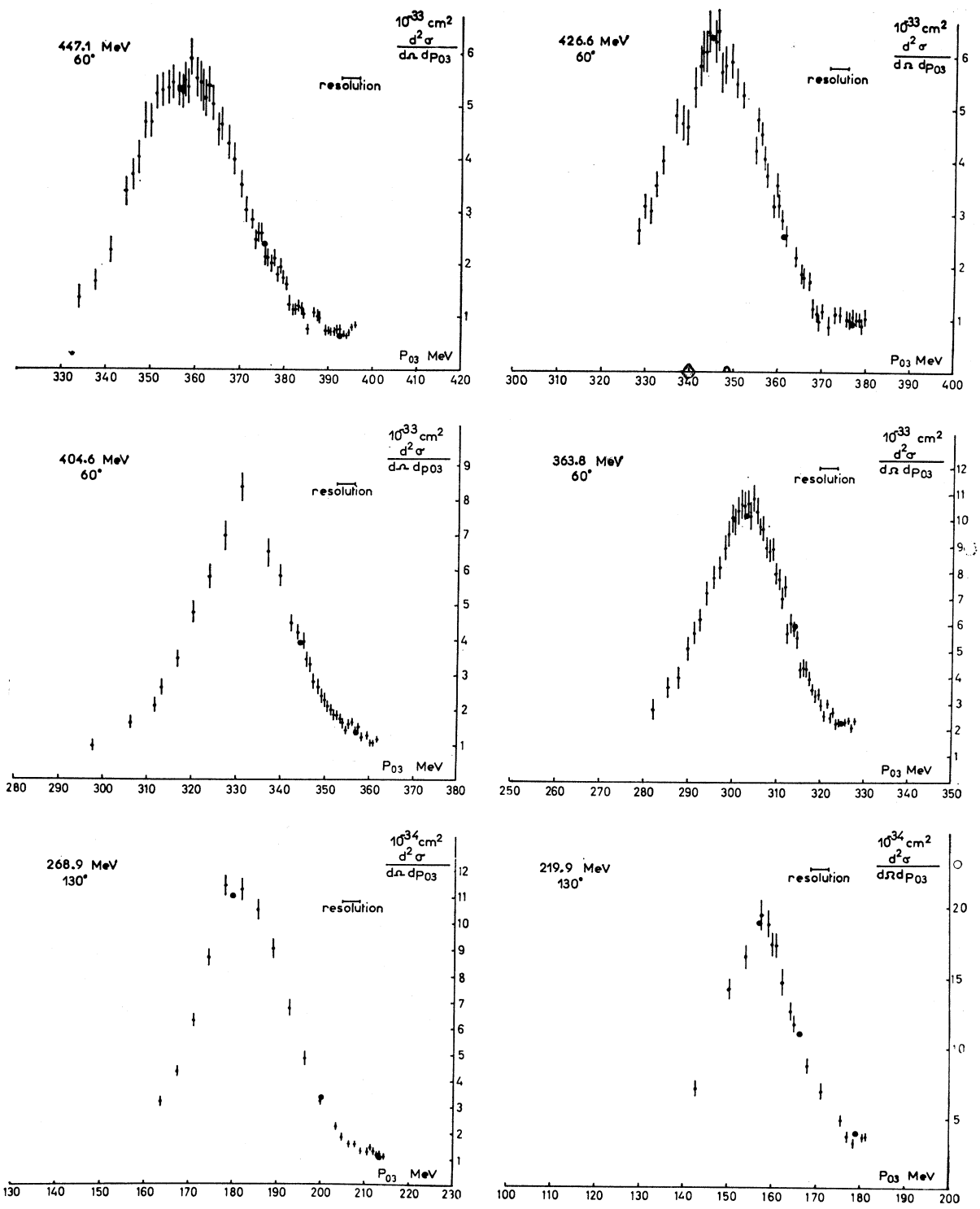

FIG. 4. Corrected spectra.

equations to obtain the right cross sections. The method used permitted us to know, in a satisfactory way, the cross-sections corrected for radiative effects. The bremsstrahlung corrections have been calculated in the same manner. It is well known that the bremsstrahlung formula is very similar to the radiative-emission formula. Thus the bremsstrahlung correction can be calculated as proportional to the radiative correction.

Because ionization involves smaller energies it is easier, using Landau's formula, to calculate the corresponding corrections.

Figure 3 shows the corrections to the inelastic data; Fig. 4 shows the corrected spectra, in which the elastic peak is not apparent, being a δ function.

For the 17 points taken with better accuracy, Table III gives numerical values of the corrections and of the cross sections. Numerical values for the other points are given in Ref. 9.

VI. ERRORS

Two series of points have been taken. First, each complete spectrum was measured with poor statistics, the statistical error being the most important. Second, 17 points were measured with a 2% statistical error. For these last points numerous tests (energy determination, beam position, monitor calibration) have been made to minimize the other errors, using the same method as in the elastic-deuteron-scattering experiments.[2] However, the spectrometer dispersion introduces an error for the inelastic scattering, whereas this error does not appear for the elastic scattering. See Table IV for numerical values of errors at the top of the inelastic peak.

TABLE IV. Errors (in percent) for the determination of the ratio of the proton cross section to the deuteron cross section at the top of the quasi-elastic peak.

Incident energy (MeV) / Scattering angle (deg)	447 / 60	427 / 60	363 / 60	267 / 130	219 / 130
Top of the quasi-elastic peak: statistical error	1.6	1.6	1.6	1.6	2.0
Charge determination, multiple scattering	0.5	0.5	0.5	0.5	1.5
Čerenkov efficiency, slits penetration, π^-	2.0	2.0	1.6	1.0	1.0
Width of the momenta slits	0.5	0.5	0.5	0.3	0.3
Spectrometer dispersion	0.5	0.5	0.5	0.5	0.5
Beam dispersion	0.3	0.3	0.3	0.3	0.3
Beam position	2.2	2.2	2.2	2.2	2.2
Density ratio of hydrogen and deuterium	0.5	0.5	0.5	0.5	0.5
Solid angle	...	0.5	...	...	0.5
Geometry errors	1	1.4	1	1	1.4
Proton cross-section: statistical error	1.4	1.4	1.3	1.4	1.4
Hydrogen impurity in deuterium	...	1.3	...	...	...
Radiative corrections	1	1	1	1	1
Total error on the ratio proton/deuteron	3.8	3.9	3.5	3.1	3.5

[9] B. Grossetête, Ref. 6.

VII. NEUTRON FORM FACTORS

From the ratio of the proton and deuteron cross-sections at the top of the inelastic peak for the 60° and 130° angles, we can calculate the neutron form factors. See discussions in the following article.[1] Here we use Durand's formula[10]:

$$\frac{d^2\sigma}{d\Omega dp_{03}}=\frac{\alpha^2}{4p_{01}^2}\frac{\cos^2(\theta/2)}{\sin^4(\theta/2)}\times\frac{(4.5\times10^{-3}\ \mathrm{MeV}^{-1})}{[(q^2/4M^2)(1+q^2/4M^2)]^{1/2}}(G_p+G_n),$$

where

$$G_{\mathrm{nucleon}}=\frac{1}{1+q^2/4M^2}\times\left\{F_c^2+\frac{q^2}{4M^2}\left[1+2\left(1+\frac{q^2}{4M^2}\right)\tan^2\frac{\theta}{2}\right]\mu^2F_m^2\right\}_c.$$

We find the results in Table V.

TABLE V. Neutron form factors.

q^2 (F^{-2})	F_m^n/F_m	$(F_c^n/F_c)^2$
2.85	1.076±0.082	−0.024±0.071
4.1	0.994±0.068	0.026±0.080

VIII. CONCLUSIONS

Using Durand's formula we find that at $q^2=2.85$ F^{-2} and $q^2=4.1$ F^{-2}, the magnetic proton form factor is almost equal to the magnetic neutron form factor. This is in agreement with the elastic-scattering results at the same q^2.[11] For the neutron-charge form factors, we are also in agreement with the elastic results; however, the values are much less accurate and we find that F_c^n is 0 within the error limit.

On the other hand, we measured the inelastic spectra at four different energies for the 60° angle and at two energies for the 130° angle. These spectra are interpreted in the following article.[1]

[10] Loyal Durand, III, Phys. Rev. **123**, 1393 (1961); Phys. Letters **13**, 184 (1964).

[11] D. Benaksas, D. J. Drickey, and D. Frèrejacque, Phys. Rev. Letters **13**, 353 (1964).